Apoptosis Induction by Plectranthus Amboinicus and Hibiscus Rosasinensis Extracts in HepG2 Cells: Insights into Cytotoxicity and Gene Regulation

Imbaasree Rajavelu[1*], Bhargavi Rajarathinam[2]

Indian Academy Degree College – Autonomous, Bengaluru, India

[*]Corresponding Author

DOI: https://dx.doi.org/10.51584/IJRIAS.2026.11010011

Received: 28 December 2025; Accepted: 04 January 2026; Published: 22 January 2026

ABSTRACT

Hepatocellular carcinoma (HCC) is a highly aggressive cancer associated with chronic liver diseases, posing significant treatment challenges. This study explores the apoptotic potential of ethanolic leaf extracts from *Plectranthus amboinicus* and *Hibiscus rosa-sinensis* on HepG2 cell lines, aiming to elucidate their mechanisms of action and comparative efficacy. Both extracts underwent phytochemical analysis, antioxidant activity assessment using the DPPH assay, and safety evaluation through haemolytic activity determination. Apoptosis was visualized using acridine orange/ethidium bromide dual staining and quantified with propidium iodide/annexin V-FITC staining and flow cytometry. The regulation of key apoptotic genes, BAX and BCL-2, was analysed in treated HepG2 cells. Preliminary results indicate that both extracts exhibit significant antioxidant activity, with *P. amboinicus* demonstrating robust effects and a favourable safety profile. In contrast, *H. rosasinensis* showed increased cytotoxicity, raising concerns regarding its therapeutic application. This comparative analysis highlights the potential of *P. amboinicus* as a promising candidate for novel HCC therapeutic strategies, while underscoring the need for further investigation into the apoptotic mechanisms and safety of *H. rosasinensis*. The *P. amboinicus* extract effectively induces apoptosis in HepG2 cells by modulating the expression of key apoptosis regulators, BAX and BCL-2, without significant haemolytic toxicity at lower concentrations. These findings provide a strong foundation for further research into the therapeutic applications of *P. amboinicus* in liver cancer treatment.

Keywords: Hepatocellular carcinoma, Plectranthus amboinicus, Hibiscus rosa-sinensis, HepG2 cell line, Ethanolic extracts, Apoptosis, Cytotoxicity, BAX, BCL-2.

INTRODUCTION

Hepatocellular carcinoma (HCC) is one of the most aggressive and rapidly progressing cancers globally, often arising from chronic liver diseases such as cirrhosis and hepatitis. These conditions create a permissive environment for carcinogenesis through complex molecular and cellular perturbations [1]. The pathogenesis of HCC is influenced by several factors, including chronic inflammation, dysregulated cellular proliferation, and impaired apoptosis [2]. A critical hallmark of HCC is the disruption of apoptotic pathways, leading to an imbalance between cell survival and programmed cell death, which fosters the progression from chronic liver injury to malignancy [3]. Apoptosis, a tightly regulated process of programmed cell death, is essential for eliminating damaged or dysfunctional cells. The BCL-2 family of proteins plays a pivotal role in this process, with pro-apoptotic members such as BAX promoting apoptosis and anti-apoptotic members like BCL-2 inhibiting it [4]. In HCC, the overexpression of anti-apoptotic proteins, coupled with the downregulation of proapoptotic counterparts, contributes to resistance to apoptosis, allowing malignant hepatocytes to evade death and continue proliferating. This apoptotic resistance not only drives tumorigenesis but also presents significant challenges for therapeutic intervention [5]. Oxidative stress, characterized by an excess of reactive oxygen species (ROS), is a critical factor in the development and progression of HCC. Elevated ROS levels can induce apoptosis through mitochondrial dysfunction and the activation of pro-apoptotic factors. However, chronic oxidative stress can also lead to cellular damage that promotes survival pathways, enabling cancer cells to evade apoptosis and contributing to tumorigenesis. Additionally, oxidative stress can cause genetic mutations and chromosomal instability, further driving the transformation of normal cells into cancerous ones [6].

Given the limitations of conventional therapies in effectively managing HCC, there is a growing interest in exploring alternative therapeutic approaches, particularly those involving bioactive compounds from natural sources [7]. Ethanolic leaf extracts of *P. amboinicus* and *H. rosa-sinensis* have emerged as promising candidates due to their potent anti-cancer and antioxidant properties [8] [9]. These extracts are rich in phytochemicals that exhibit robust antioxidant activity, which may play a critical role in mitigating oxidative stress—a key driver of HCC pathogenesis. While *H. rosa-sinensis* has shown potential in inducing apoptosis, preliminary findings suggest that its cytotoxic effects may be more pronounced, necessitating a comparative evaluation with *P. amboinicus*. The aim of this project is to evaluate the apoptotic potential of both *H. rosa-sinensis* and *P. amboinicus* extracts on HepG2 cell lines, a widely used in vitro model for liver cancer research.

The aim of this research is to evaluate the apoptotic potential of *H. rosa-sinensis* and *Plecanthrus ambonicus* extracts on HepG2 cell line. The objectives of the project are as follows:

1) Extraction of phytochemicals from the plant material. 2) Phytochemical analysis of plant extract to screen for potential apoptotic substances. 3) Estimation of antioxidant potential of plant extracts using DPPH free radical scavenging assay. 4) Determination of Haemolytic activity of plant extracts. 5) Acridine orange and Ethidium bromide dual staining using HepG2 cell line. 6) Apoptosis detection using pi annexin V-FITC staining of HepG2 cells by flow cytometry. 7) Gene regulation of BAX and bcl2 genes in HEP- G2 cells treated with test samples.

By elucidating the apoptotic mechanisms induced by both *P. amboinicus* and *H. rosa-sinensis*, this study aspires to contribute to the development of novel, more effective therapeutic strategies for HCC, potentially offering alternative, less toxic treatment options for this challenging malignancy.

MATERIAL AND METHODS

Collection and Propagation of Plant Material

Leaves from the plants were collected at The University of Trans-Disciplinary Health Sciences and Technology (TDU). The plant material was thoroughly washed with tap water and then shade-dried at room temperature until all moisture was completely removed. Once dried, the plant material was ground into a fine powder.

Preparation of Plant Material and Extraction

A total of 20 g of the dried powdered sample was dissolved in 100 ml of ethanol in a 500 ml beaker. The beaker containing the dissolved sample was covered with aluminum foil and placed in a hot water bath at 50ºC for 4 hours. After the incubation period, the extract was filtered using Whatman filter paper, and the filtrate was collected in a 50 ml beaker. The residue on the filter paper was discarded, and the filtrate was retained for further use. The filtrate was then kept at 50ºC for several hours until it completely dried and formed a semi-solid substance. The weight of the semi-solid extract was recorded, and the yield was noted [10].

Phytochemical Analysis

Test for Alkaloids: Dragendoff's Test

To 0.2 ml of the sample, 0.2 ml of hydrochloric acid (HCl) was added, followed by 2-3 drops of Dragendoff's reagent. The appearance of an orange or red precipitate, along with a turbid solution, indicates the presence of alkaloids [11].

Test for Carbohydrates: Molisch's Test

A mixture of 0.2 ml of the sample and a few drops of Molisch's reagent (α-naphthol dissolved in alcohol) was prepared. To this mixture, 0.2 ml of sulfuric acid was carefully added along the sides of the test tube. A positive test is indicated by the formation of a purple color ring [12].

Test for Tannins: Braymer's Test

To 0.2 ml of the plant extract, 2 ml of water was added and heated in a water bath for 10 minutes. The mixture was then filtered, and ferric chloride was added to the filtrate. The appearance of a dark green solution indicates the presence of tannins [13].

ISSN No. 2454-6194 | DOI: 10.51584/IJRIAS |Volume XI Issue I January 2026

Test for Terpenoids: Salkowski's Test

In a test tube, 0.2 ml of the plant extract was mixed with 0.2 ml of chloroform. Concentrated sulfuric acid was carefully added to form a distinct layer. The presence of terpenoids is indicated by a reddish color at the interface [13][14].

Test for Glycosides

To 0.2 ml of the sample, 0.2 ml of chloroform and 0.2 ml of acetic acid were added, and the mixture was cooled on ice. Concentrated sulfuric acid was then carefully added, and a color change from violet to blue to green indicates the presence of a steroidal nucleus, which is part of the glycoside [13].

Test for Steroids: Lieberman-Burchardt Test

A mixture of 0.2 ml of the extract and 0.2 ml of chloroform was prepared. To this, 0.2 ml of concentrated sulfuric acid was added, and the appearance of a red color in the lower layer of chloroform indicates the presence of steroids [15].

Test for Saponins: Foam Test

To 0.2 ml of the extract, 0.6 ml of water was added in a test tube. The mixture was shaken vigorously, and the formation of persistent foam confirms the presence of saponins [13].

Test for Flavonoids: Alkaline Reagent Test

In a test tube, 0.2 ml of the extract was mixed with dilute sodium hydroxide solution. Dilute hydrochloric acid was then added. The observation of a yellow solution that later turns colorless indicates the presence of flavonoids [16].

Mucilage Test (Glycoprotein)

To 0.2 ml of the extract, 0.2 ml of absolute alcohol was added and allowed to dry. The occurrence of precipitation indicates the presence of mucilage [17].

Test for Volatile Oils

To 0.2 ml of the extract, a few drops of dilute hydrochloric acid were added. The appearance of a white precipitate indicates the presence of volatile oils [18].

Test for Phenols

To 0.2 ml of the extract, 0.4 ml of distilled water and a few drops of 10% aqueous ferric chloride solution were added. The formation of a blue or green color indicates the presence of phenols [13].

DPPH Assay:

The DPPH radical scavenging assay was performed. Briefly, 80 µl of DPPH solution (EEC No. 217-591-8,

Sigma, USA) and various concentrations of the test solution were combined with HPLC grade methanol

(Ranbaxy Chemicals) to a final volume of 240 µl. The reference standard was tested at concentrations of 0.3125, 0.625, 1.25, 2.5, 5, and 10 µg/ml. The reaction mixture was vortexed and incubated at 25°C for 15 minutes. The absorbance was measured at 510 nm using a semi-autoanalyzer. A control reaction was carried out without the test sample [19].

MTT Assay:

The purpose of this SOP is to provide clear and concise instructions on performing cytotoxicity assay by MTT method. For the standard, a 10 mM stock solution of Doxorubicin was prepared, followed by serial two-fold dilutions from 100 µM to 3.125 µM using DMEM plain media. For sample preparation in cytotoxicity studies, 32 mg/ml stocks were prepared using DMSO, with serial two-fold dilutions made from 320 µg/ml to 10 µg/ml using DMEM plain media [20].

ISSN No. 2454-6194 | DOI: 10.51584/IJRIAS |Volume XI Issue I January 2026

Cell lines and culture medium:

HepG2 cell lines were procured from ATCC and cultured in DMEM supplemented with 10% inactivated fetal bovine serum (FBS), penicillin (100 IU/ml), and streptomycin (100 µg/ml) in a humidified atmosphere of 5% CO_2 at 37 °C until confluent. Cells were dissociated using a cell dissociation solution (0.2% trypsin, 0.02% EDTA, 0.05% glucose in PBS). Cell viability was assessed, and cells were centrifuged. A total of 50,000 cells per well were seeded in a 96-well plate and incubated for 24 hours at 37 °C in a 5% CO_2 incubator. The monolayer cell culture was trypsinized, and the cell count was adjusted to 5.0 x 10^5 cells/ml using media containing 10% FBS. To each well of a 96-well microtiter plate, 100 µl of the diluted cell suspension (50,000 cells/well) was added. After 24 hours, the supernatant was removed, and the monolayer was washed once with medium. Different test concentrations of the drugs were added to the wells containing the partial monolayer, and the plates were incubated at 37 °C for 24 hours in a 5% CO_2 atmosphere. After incubation, the test solutions were discarded, and 100 µl of MTT (5 mg/10 ml in PBS) was added to each well. The plates were incubated for 4 hours at 37 °C in a 5% CO_2 atmosphere. The supernatant was then removed, and 100 µl of DMSO was added to each well to solubilize the formazan crystals. The absorbance was measured using a microplate reader at a wavelength of 590 nm.
The percentage of growth inhibition was calculated using the formula:

$$\%\ Inhibition = \frac{OD\ of\ Control - OD\ of\ Sample}{OD\ of\ Control}\ X\ 100$$

The concentration of the test drug required to inhibit cell growth by 50% (IC_{50}) values was generated from the dose-response curves for each cell line [21].

HepG2 cell lines were procured from ATCC and cultured in DMEM supplemented with 10% inactivated fetal bovine serum (FBS), penicillin (100 IU/ml), and streptomycin (100 µg/ml) in a humidified atmosphere of 5% CO_2 at 37 °C until confluent. Cells were dissociated using a cell dissociation solution (0.2% trypsin, 0.02%

EDTA, 0.05% glucose in PBS). Cell viability was assessed, and cells were centrifuged. A total of 50,000 cells

$$\%\ Inhibition = \frac{OD\ of\ Control - OD\ of\ Sample}{OD\ of\ Control}\ X\ 100$$

Haemolysis:

Five milliliters of blood was collected from healthy volunteers in tubes containing 5.4 mg of EDTA to prevent coagulation. The blood samples were centrifuged at 1000 rpm for 10 minutes at 4°C. The plasma was carefully removed, and the white buffy layer was fully eliminated by aspiration using a pipette with utmost care. The erythrocytes were then washed three times with 1X PBS (pH 7.4). The thoroughly washed erythrocytes were stored at 4°C and used within 6 hours to conduct the hemolysis assay [22].

An erythrocyte suspension was prepared by diluting 100 µl of erythrocytes in 900 µl of 1X PBS, resulting in a 10-fold dilution. A volume of 50 µl of this diluted erythrocyte suspension was taken into 2 ml Eppendorf tubes. To these tubes, 100 µl of the test samples (plant extracts, compounds, etc.) were added. As a negative control, 100 µl of 1X PBS was used, and 100 µl of 1% Triton X-100 or 1% SDS served as a positive control. The reaction mixture was then incubated at 37°C for 60 minutes [23]. The volume of the reaction mixture was adjusted to 1 ml by adding 850 µl of 1X PBS. This reaction mixture was finally centrifuged at 300 rpm for 3 minutes, and the resulting supernatant containing hemoglobin was measured at 540 nm using a spectrophotometer to determine the hemoglobin concentration [24].

The percentage of hemolysis was calculated using the following formula:

$$\%\ Haemolysis = \frac{(Control\ OD - Sample\ OD)}{Control\ OD}\ X\ 100$$

ISSN No. 2454-6194 | DOI: 10.51584/IJRIAS |Volume XI Issue I January 2026

Acridine Orange and Ethidium Bromide Dual Staining:

Twenty-five microliters (approximately 1 x 10^5 cells) of treated and untreated cells were placed in separate microcentrifuge tubes and stained with 5 µl of Acridine Orange-Ethidium Bromide (AO-EtBr) for about 2 minutes, followed by gentle mixing. A 10 µl aliquot of the cell suspension was then placed onto a microscopic slide and covered with a glass coverslip for examination under a fluorescence microscope using a fluorescein filter. The magnification should be adjusted as needed based on the cell type to ensure that nuclear morphology is discernible [25].

Flow Cytometry Method:

The day before inducing apoptosis, 1 x 10^6 cells were plated per well in a 6-well plate using DMEM cell culture medium. After approximately 18 hours, floating (dead) cells were removed by pipetting, and fresh culture medium was added to restore the original volume. The treated cells were then exposed to 80 and 160 µg/ml of three different samples to induce apoptosis and incubated for 24 hours. Following this, the cell culture medium was collected into 15 mL tubes. The cells were detached from the dish using a cell scraper, and 1 mL of medium was added to each well before transferring the contents to the 15 mL tubes. The samples were centrifuged, and the supernatant was discarded. The cells were washed twice with cold PBS and then resuspended in 1 mL of 1X Binding Buffer at a concentration of approximately 1 x 10^6 cells/mL.For flow cytometry analysis, 500 µl of the cell suspension was aliquoted, and 10 µl of propidium iodide (PI) and 5 µl of Annexin V were added. The suspension was incubated for 15 minutes at room temperature in the dark. After incubation, the cells were analyzed by flow cytometry as soon as possible (within 1 hour [26][27].

Gene Regulation of BAX and BCL2 Genes in HEPG2 cells treated with given samples:

Treatments:

Table 1: Treatment of HepG2 cell lines with the Plecthranthus amboinicus at treatment concentrations of 80 µg/ml and 160 µg/ml.

Sample	Treatment (µg/ml)	Treatment condition
Control	0 (Media)	HEP-G2 cells (1× 10^6) grown in P35 dish were treated with test compound for 24 hours
Plecthranthus amboinicus	80	
	160	

Sample preparation and RNA isolation:

Total RNA was extracted from HepG2 cells using TRIzol Reagent (Invitrogen, catalog numbers 15596026 and 15596018) following the manufacturer's instructions. The HepG2 cells were washed twice with PBS and then centrifuged at 2000 rpm for 5 minutes. To the resulting cell pellet, 0.5 ml of TRIzol was added in a 1.5 ml centrifuge tube and vortexed thoroughly. The samples were allowed to stand at room temperature for 5 minutes. Next, 0.2 ml of chloroform (CAS No. 67-66-3) was added, and the mixture was vigorously shaken for 15 seconds. The tube was then incubated at room temperature for an additional 5 minutes and centrifuged at 10,000 rpm for 15 minutes at 4°C. The upper aqueous phase was carefully transferred to a new sterile microcentrifuge tube and treated with 0.5 ml of isopropanol (CAS No. 63-67-0). This mixture was gently inverted five times and incubated at room temperature for 5 minutes. Subsequently, the samples were centrifuged at 10,000 rpm for 10 minutes at 4°C. The supernatant was discarded, and the RNA pellet was washed by adding 1 ml of 70% ethanol. The sample was mixed gently by inverting it a few times and then centrifuged for 5 minutes at 14,000 rpm at 4°C. The supernatant was removed by inverting the tube on clean tissue paper, and the pellet was dried at 55°C. Finally, the RNA pellet was re-suspended in 25 µl of DEPC-treated water [28].

RT-PCR:

A semi-quantitative reverse transcriptase polymerase chain reaction (RT-PCR) was performed using the Techno Prime system to assess the mRNA expression levels of BAX, BCL2, and GAPDH. cDNA was synthesized from 2 µg of RNA using the Verso cDNA synthesis kit (Thermo Fisher Scientific) with oligo dT primer, following the

ISSN No. 2454-6194 | DOI: 10.51584/IJRIAS |Volume XI Issue I January 2026

manufacturer's instructions. The reaction volume was set to 20 µl, and cDNA synthesis was conducted at 42°C for 60 minutes, followed by inactivation of the reverse transcriptase at 85°C for 5 minutes [29].

Primers:

Table 2: Primers utilized in RT-PCR

Gene	Primer Pair	Sequence	Tm	Product size (bp)
GAPDH	FP	ACATCATCCCTGCCTCTAC	56.7	154
	RP	GGCAGGTTTTTCTAGACGG	56.7	
BAX	FP	GACACCTGAGCTGACCITGG	61	154
	RP	GAGGAAGTCCAGTGTCCAGC	61	
BCL2	FP	CTGGTGGACAACATCGCTCTG	61	150
	RP	GGTCTGCTGACCTCACTTGTG	61	

PCR:

The PCR mixture, with a final volume of 20 µL, consisted of 1 µL of cDNA and 10 µL of 2x Red Taq Master Mix (Amplicon). The samples were denatured at 94°C for 5 minutes and then amplified using 35 cycles at 94°C for 30 seconds, 53°C for 30 seconds, and 72°C for 1 minute for BAX and BCL2. The renaturation temperature for BAX and BCL2 was set to 49°C, while for GAPDH, it was set to 55°C for 30 seconds. The renaturation temperature for BAX and BCL2 was adjusted to 56°C, followed by a final elongation step at 72°C for 10 minutes. The optimal number of cycles was determined experimentally to ensure that the amplifications were within the exponential range and had not yet reached a plateau. Ten microliters of the final amplification product were loaded onto a 2% ethidium bromide-stained agarose gel and photographed. The results were quantified by measuring the optical density of the bands using the ImageJ software. The values were normalized to the intensity levels of GAPDH [30].

RESULTS

Extraction of plant samples

The plant extract was extracted using distillation method with ethanol as a solvent and the semi solid extract was weighed and the yield was noted as given below in table 3

Table 3: Yield summary after crude extraction

Sample	Amount of sample taken for extraction	Solubility	Yield
P. ambonicus	20g	EtOH	849.6mg
H. rosa-sinensis	20g	EtOH	395.4mg

Phytochemical analysis

The phytochemical analysis of ethanolic extract of the plants revealed the presence of a number of potential antioxidants and anti-cancer compounds like saponins, terpenoids, flavonoids and a few numbers of sterols which are represented in the table 4 below

Table 4: Result summary of phytochemical analysis

TYPES OF TESTS	Hibiscus	Plecanthrus
Alkaloid	+	+
Carbohydrate	+	+
Tannin	+	+
Terpenoid	-	+

ISSN No. 2454-6194 | DOI: 10.51584/IJRIAS |Volume XI Issue I January 2026

Glycoside	-	+
Steroid	-	-
Saponin	+	-
Flavonoid	-	+
Myllon's test	-	-
Glycoprotein test	-	-
Volatile oil	+	+

Note: 1. +: Positive 2. -: Negative

Based on the phytochemical analysis, both plant samples were found to contain alkaloids, carbohydrates, tannins, and volatile oils. Additionally, terpenoids, glycosides, and flavonoids were detected in *P. amboinicus*, while saponins were present in *H. rosa-sinensis*.

DPPH Assay:

In the present study, the DPPH free radical scavenging activity of the plant extracts was investigated, and the percentage inhibition along with IC50 values were calculated, as shown in Table 5 below.

Table 5: % inhibition and IC_{50} values of plant extracts and control at different concentrations

Sample	Conc (µg/ml)	OD @ 510nm	% Inhibition	IC50 (µg/ml)
C	0	0.588	0.00	**2.865**
Quercetin	0.3125	0.521	11.39	
	0.625	0.43	26.87	
	1.25	0.391	33.50	
	2.5	0.324	44.90	
	5	0.224	61.90	
	10	0.1451	75.32	
P. ambonicus	3.125	0.538	8.50	**72.42**
	6.25	0.499	15.14	
	12.5	0.454	22.79	
	25	0.422	28.23	
	50	0.386	34.35	
	100	0.28	52.38	
H. rosa-sinensis	3.125	0.569	3.23	**31.22**
	6.25	0.495	15.82	
	12.5	0.444	24.49	
	25	0.409	30.44	
	50	0.267	54.59	
	100	0.222	62.24	

From Table 5, the percentage inhibition of *P. amboinicus* at concentrations of 12.5, 25, 50, and 100 µg/ml ranged from 22% to 52%, while for *H. rosa-sinensis*, the inhibition at the same concentrations ranged from 24% to 62%. The ethanolic extracts of both plants exhibited the highest percentage of inhibition at 100 µg/ml, with values between 52.38% and 62.24%. Among these, *H. rosa-sinensis* showed the highest inhibition at 62.24%.

Graph 1 below presents a comparative analysis of the DPPH scavenging activity of the two plants. When compared to the standard quercetin, both plant extracts demonstrated at least 50% of quercetin's inhibitory capacity, highlighting their potential for therapeutic development in cancer treatment. The graph further illustrates the percentage inhibition of the plant extracts.

ISSN No. 2454-6194 | DOI: 10.51584/IJRIAS |Volume XI Issue I January 2026

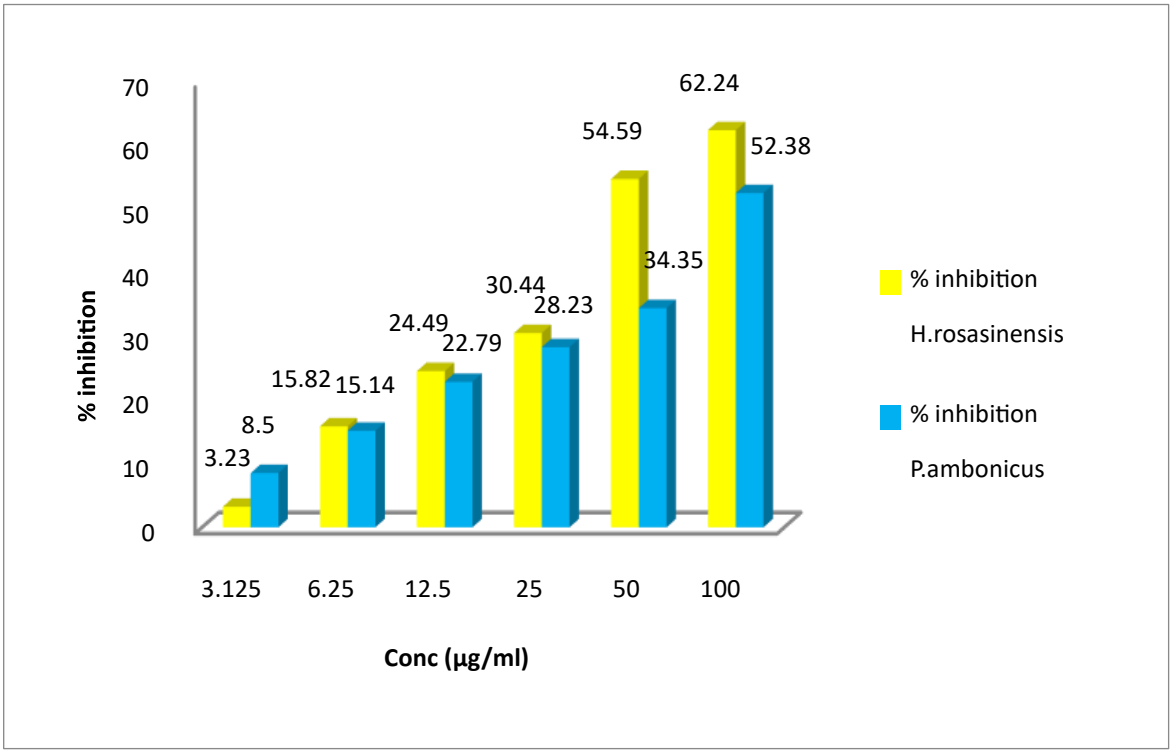

Graph 1: bar graph comparing the %inhibition of the 2 plants

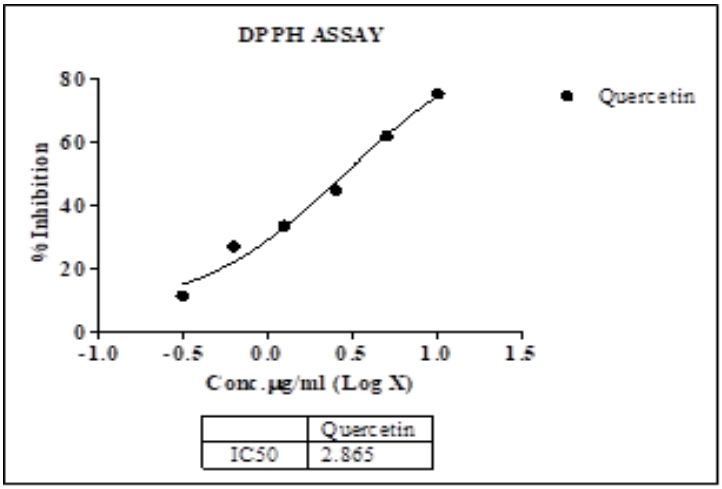

Graph 2: IC_{50} plot depicting concentration in x-axis and %inhibition on the y-axis and displaying the equations of logarithmic curves.

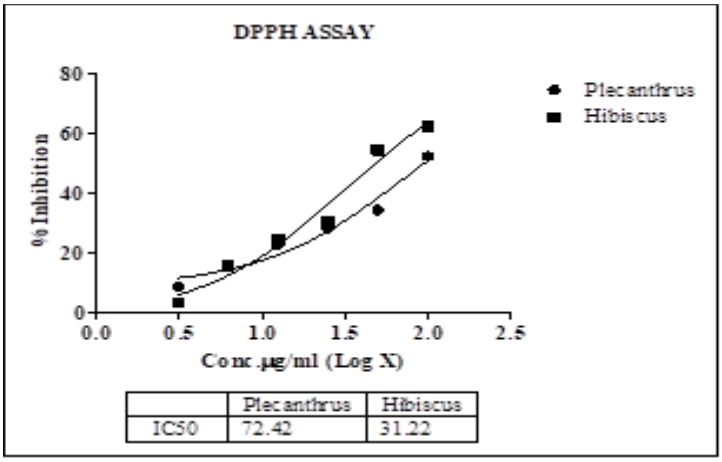

Graph 3: IC_{50} plot depicting concentration in x-axis and %inhibition on the y-axis and displaying the equations of logarithmic curves.

ISSN No. 2454-6194 | DOI: 10.51584/IJRIAS |Volume XI Issue I January 2026

The IC_{50} of each extract was calculated by using Graphpad prism by plotting log (concentration) in the x axis and the % inhibition in the y axis and a logarithmic graph 2 and 3 represents plotted IC_{50} of quercetin = 2.865 µg/ml.; *Plecthranthus ambonicus* = 72.42 µg/ml; *H. rosa-sinensis* = 31.22 µg/ml. The IC_{50} of *H. rosa-sinensis* was lowest when compared to standard quercetin.

Cytotoxicity studies for HepG-2 cell line

Cytotoxicity studies were conducted using MTT assay to measure the cytotoxic effect of the ethanolic leaves extracts of samples against the standard drug Doxorubicin on HepG-2 cell line and about 50,000 cells /well was seeded in a 96 well plate and incubated for 24 hrs. In the table 6 the percentage of inhibition of Doxorubicin for the concentration of 12.5, 25, 50 and 100µg/ml was calculated which is in the range 47-80%. In graph 4 the IC_{50} of doxorubicin was calculated by plotting log (concentration) in the x axis and the % inhibition in the y axis and logarithmic graph which is 18.26 µM.

Table 6: % inhibition and IC_{50} values of standard drug doxorubicin at different concentrations

HepG-2	**Standard**			
Compound Name	**Conc. µM**	**OD @ 590nm**	**% Inhibition**	**IC_{50} in µM**
Control	0	0.995	0.00	18.26
Doxorubicin	3.13	0.709	28.69	
	6.25	0.641	35.59	
	12.5	0.519	47.80	
	25	0.388	60.99	
	50	0.315	68.33	
	100	0.197	80.19	

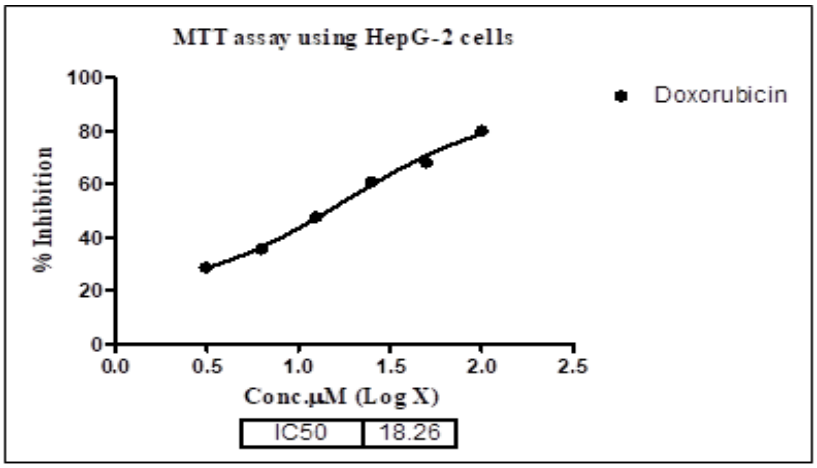

Graph 4: IC_{50} plot depicting concentration in x-axis and % inhibition on the y axis and displaying the equations of logarithmic c

urves

Table 7: %inhibition and IC_{50} values of plant extracts and control at different concentrations

HepG-2				
Compound Name	**Conc. µg/ml**	**OD @590nm**	**% Inhibition**	**IC50 µg/ml**
Control	0	0.995	0.00	
Plecthranthus amboinicus	10	0.843	15.27	146.80
	20	0.793	20.23	
	40	0.705	29.08	
	80	0.622	37.48	

ISSN No. 2454-6194 | DOI: 10.51584/IJRIAS |Volume XI Issue I January 2026

	160	0.478	51.92	
	320	0.349	64.94	
Hibiscus rosa-sinensis	10	0.854	14.17	278.20
	20	0.801	19.45	
	40	0.749	24.73	
	80	0.668	32.82	
	160	0.607	39.00	
	320	0.433	56.47	

The concentration of sample, OD reading at 590nm, % inhibition and the IC_{50} values are calculated which are represented in table 7. The percentage of inhibition of *Plecthranthus amboinicus* and *H. rosa-sinensis* for the concentration of 10, 20, 40, 80, 160 and 320µg/ml was calculated which is in the range 15-64% and 14-56% respectively. In the graph 5 the IC_{50} of *Plecthranthus amboinicus* and *H. rosa-sinensis* was calculated by plotting log (concentration) in the x axis and the % inhibition in the y axis and logarithmic graph which is 146.80µg/ml and 278.20 µg/ml respectively.

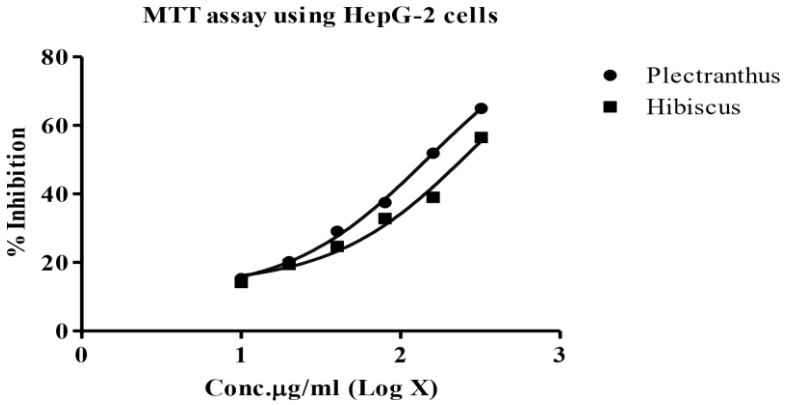

	Plectranthus	Hibiscus
IC50	146.8	278.2

Graph 5: IC_{50} plot depicting concentration in x-axis and % inhibition on the y axis and displaying the equations of logarithmic curves

Results showed that *Plecthranthus amboinicus* induced statistically significant increase in the inhibition value of HepG2 cells in a concentration dependent manner. The ethanolic extracts of both plants showed maximum % of inhibition at concentration of 100 µg/ml. Out of these, extract *Plecthranthus amboinicus* showed maximum % inhibition. The IC_{50} of *Plecthranthus amboinicus* was lowest when compared to standard doxorubicin.

Determination of Haemolysis activity

In vitro hemolytic activity on human erythrocytes of ethanolic extracts obtained from leaves of *Plecthranthus amboinicus* and *H. rosa-sinensis* was performed. The results of haemolysis induced by ethanolic leaves extracts of the samples at the concentration of 10, 20, 40, 80, 160, and 320 µg/ml whose percentage haemolytic activity is summarized in Table 8.

Table 8: % Hemolysis values of plant extracts and control at different concentrations

Sample	**Treatment**	**Absorbance**	**% Haemolysis**
Control	PBS (100 µl)	0.561	0.00
Positive control	1% SDS (100 µl)	0.103	81.64
Plecthranthus ambonicus	10	0.482	14.08
	20	0.444	20.86
	40	0.416	25.85

	80	0.412	26.55
	160	0.399	28.87
	320	0.321	42.78
H. rosa-sinensis	10	0.464	17.29
	20	0.433	22.82
	40	0.404	27.99
	80	0.371	33.87
	160	0.347	38.15
	320	0.307	45.28

From Table 8, the percentage of hemolytic activity for *P. amboinicus* at concentrations of 10, 20, 40, 80, 160, and 320 µg/ml ranged from 14% to 42%, while for *H. rosa-sinensis*, the hemolytic activity at the same concentrations ranged from 17% to 45%. The ethanolic extracts of both plants exhibited the highest percentage of hemolytic activity at a concentration of 320 µg/ml, indicating significant hemolytic activity at higher concentrations.

The hemolysis test results suggest that *H. rosa-sinensis* at concentrations of 10, 20, and 40 µg/ml is considered safe for pharmacological use, while concentrations of 80, 160, and 320 µg/ml are considered toxic, as they cause 30% hemolysis in RBCs. In contrast, *P. ambonicus* extract at concentrations of 10, 20, 40, 80, 160, and 320 µg/ml is deemed safe for pharmacological use, as it results in less than 30% hemolysis.

Acridine Orange and Ethidium Bromide dual staining studies using HepG2 cell line

Apoptosis studies were conducted to assess the ability of the test compounds to induce apoptosis in HepG2 cell lines.

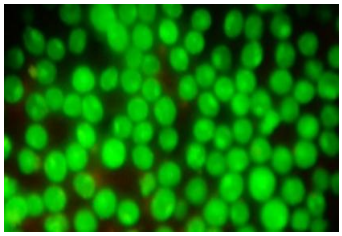

Fig: 1

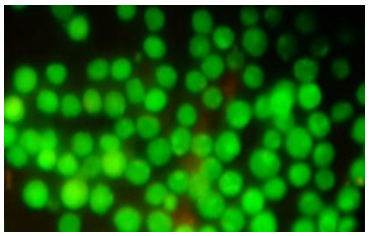

Fig: 2

Control HepG2 cells

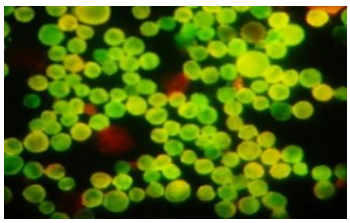

Fig: 3

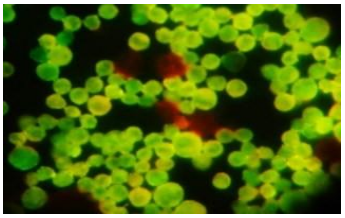

Fig: 4

Sample *P. ambonicus*-80µg/ml

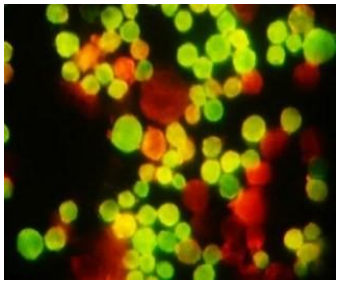

Fig: 5

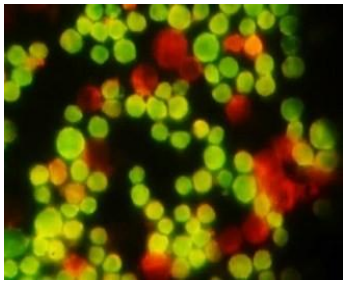

Fig: 6

ISSN No. 2454-6194 | DOI: 10.51584/IJRIAS |Volume XI Issue I January 2026

Sample *P. ambonicus* -160µg/ml

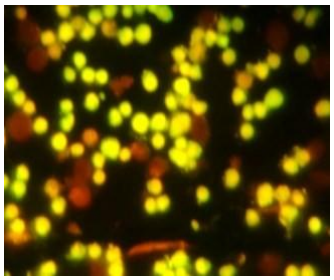

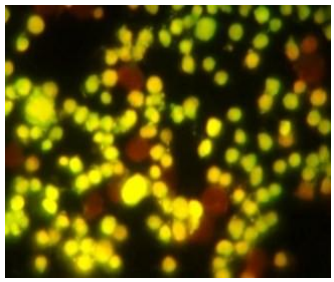

Fig: 7 **Fig: 8**

Standard Doxorubicin-25µM

Dual staining was performed and examined under a fluorescent microscope. In the control group (Figures 1 and 2), normal cells display a circular nucleus uniformly distributed in the center of the cell. Figures 3 and 4 show early-stage apoptotic cells, where the cell nuclei exhibit yellow-green fluorescence due to Acridine Orange (AO) staining, with the nuclei concentrated into a crescent or granular shape located on one side of the cells. The staining is asymmetrically localized within the cells. In Figures 5 and 6, the nuclei of the cells show orange fluorescence from EtBr staining, indicating the late apoptotic phase, with the nuclei concentrated and biased to one side. Cells that have fully taken up EtBr, as seen in Figures 7 and 8, are identified as necrotic cells.

Apoptosis detection using PI Annexin V-FITC staining of HepG2 cells by Flow Cytometry

Figures 9, 10, 11, and 12 from the flow cytometry assay were generated using BD FACS Calibre software, which was also utilized to calculate the percentage of apoptosis induced by the *Plecthranthus amboinicus* leaves extract in HepG2 cell lines.

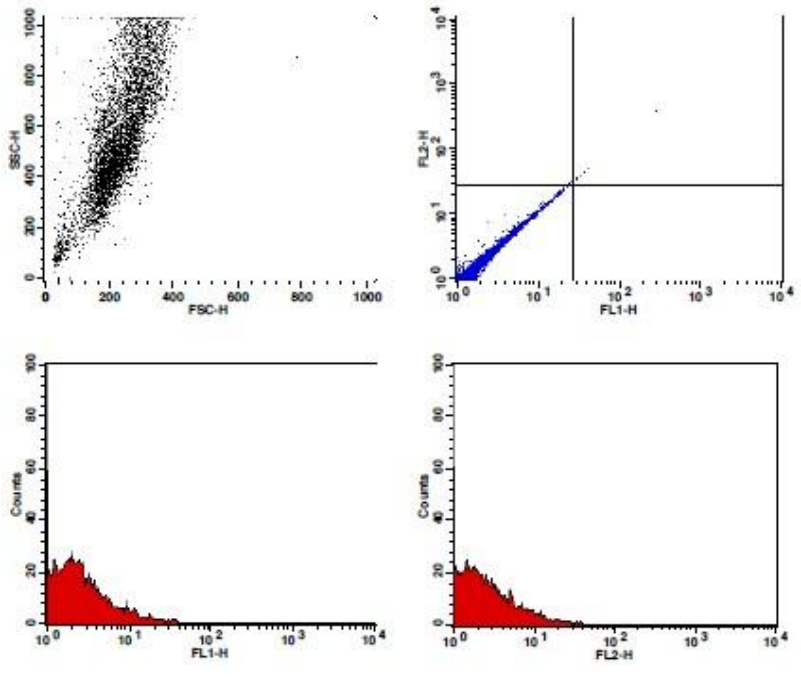

Quadrant Statistics

Quad	Events	% Gated	% Total	X Mean	Y Mean
UL	2	0.04	0.04	26.18	28.90
UR	12	0.24	0.24	55.21	64.64
LL	4986	99.72	99.72	2.74	2.59
LR	0	0.00	0.00	***	***

Figure 9: HepG2 untreated cells

In figure 9 four graph is obtained. the first graph obtained shows the scattered cells in the form of black dots which represents the cells taken up by instrument, the second graph shows four quadrants representing the

ISSN No. 2454-6194 | DOI: 10.51584/IJRIAS |Volume XI Issue I January 2026

scattering of viable, apoptotic and necrotic cells, wherein the upper left quadrant represents the necrotic cells (0.04%), the upper right quadrant represents the late apoptotic cells (0.24%), the lower right quadrant represents early apoptotic cells (0%) and the lower left represents the viable cells (99.72%). The third and fourth graph is the histogram representation of first and second graph respectively.

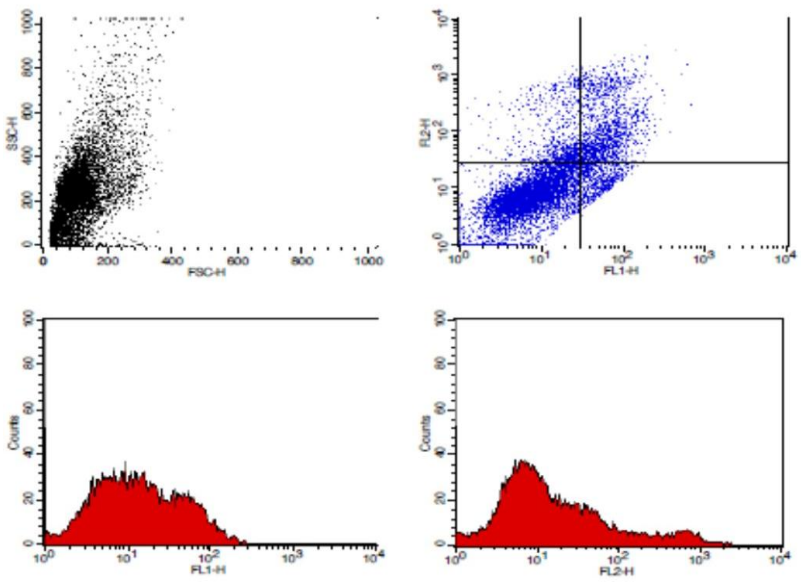

Quadrant Statistics

Quad	Events	% Gated	% Total	X Mean	Y Mean
UL	813	8.13	8.13	17.56	161.26
UR	1836	18.36	18.36	70.69	231.27
LL	6594	65.94	65.94	8.58	7.65
LR	757	7.57	7.57	53.88	15.35

Figure 10: HepG2 cells treated with sample *P. ambonicus* 80µg/ml

In figure 10 four graph is obtained. the first graph obtained shows the scattered cells in the form of black dots which represents the cells taken up by instrument, the second graph shows four quadrants representing the scattering of viable, apoptotic and necrotic cells, wherein the upper left quadrant represents the necrotic cells (8.13%), the upper right quadrant represents the late apoptotic cells (18.36%), the lower right quadrant represents early apoptotic cells (7.57%) and the lower left represents the viable cells (65.94%). The third and fourth graph is the histogram representation of first and second graph respectively.

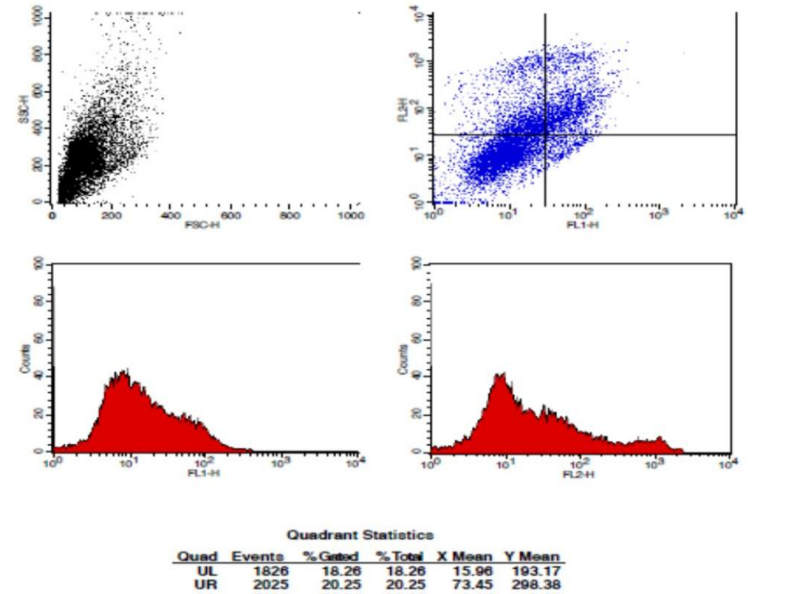

Quadrant Statistics

Quad	Events	% Gated	% Total	X Mean	Y Mean
UL	1826	18.26	18.26	15.96	193.17
UR	2025	20.25	20.25	73.45	298.38
LL	5632	56.32	56.32	8.95	9.92
LR	517	5.17	5.17	57.34	16.56

Figure 11: HepG2 cells treated with sample *P. ambonicus* 160µg/ml

ISSN No. 2454-6194 | DOI: 10.51584/IJRIAS |Volume XI Issue I January 2026

In figure 11 four graph is obtained. the first graph obtained shows the scattered cells in the form of black dots which represents the cells taken up by instrument, the second graph shows four quadrants representing the scattering of viable, apoptotic and necrotic cells, wherein the upper left quadrant represents the necrotic cells (18.26%), the upper right quadrant represents the late apoptotic cells (20.25%), the lower right quadrant represents early apoptotic cells (5.17%) and the lower left represents the viable cells (56.32%). The third and fourth graph is the histogram representation of first and second graph respectively.

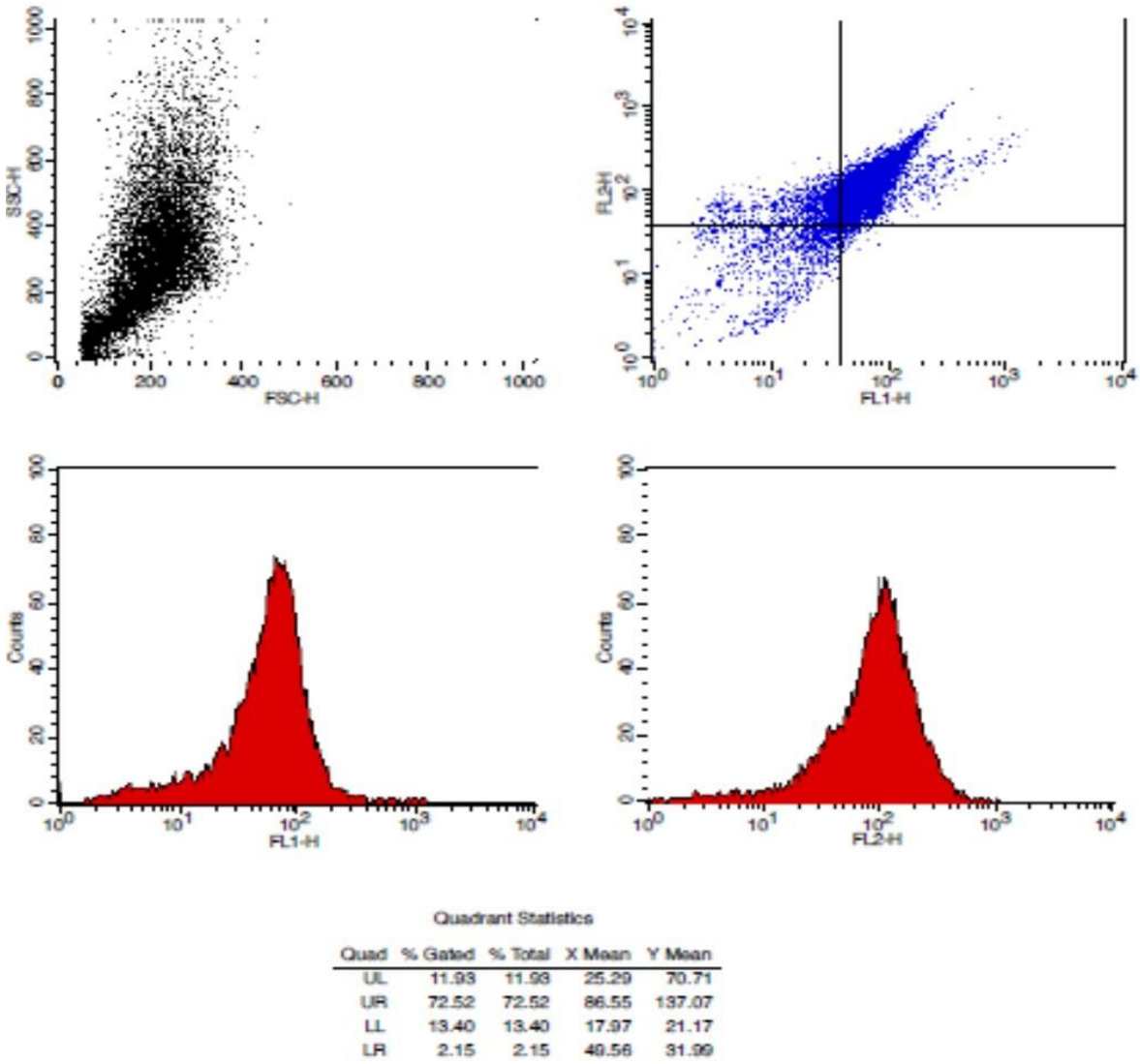

Figure 12: HepG2 cells treated with standard Doxorubicin 25µM

In figure 12, four graphs are obtained. the first graph obtained shows the scattered cells in the form of black dots which represents the cells taken up by instrument, the second graph shows four quadrants representing the scattering of viable, apoptotic and necrotic cells, wherein the upper left quadrant represents the necrotic cells (11.93%), the upper right quadrant represents the late apoptotic cells (72.52%), the lower right quadrant represents early apoptotic cells (2.15%) and the lower left represents the viable cells (13.40%). The third and fourth graph is the histogram representation of first and second graph respectively.

Table 9: Flow cytometry analysis of Apoptosis detection of HepG2 cells

Cell Line	Sample (µg/ml)	Viable Cells (%)	Early Apoptotic (%)	Late Apoptotic (%)	Necrotic Cells (%)
HepG2	Control	99.72	0.00	0.24	0.04
HepG2	*Plectranthus* (80 µg/ml)	65.94	7.57	18.36	8.13
HepG2	*Plectranthus* (160 µg/ml)	56.32	5.17	20.25	18.26
HepG2	Doxorubicin (25 µM)	13.40	2.15	72.52	11.93

ISSN No. 2454-6194 | DOI: 10.51584/IJRIAS |Volume XI Issue I January 2026

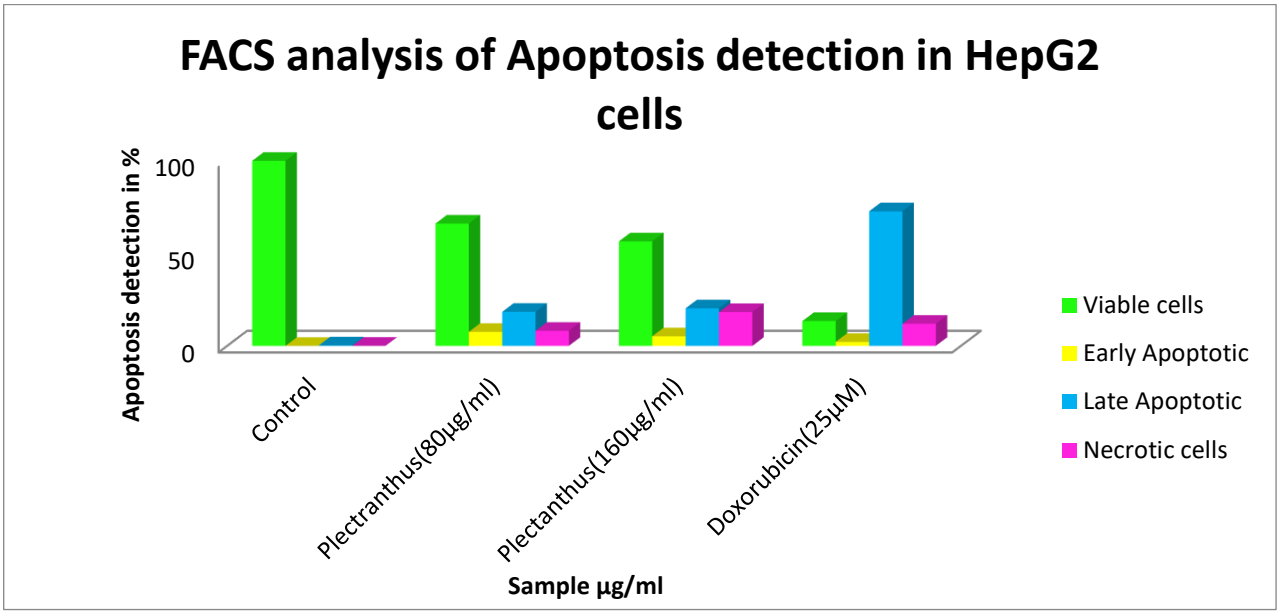

Figure 13: FACS analysis of Apoptosis detection in HepG2 cells

The table 9 and figure 13 represents the FACS analysis of apoptosis detection in HepG2 cell lines. From the flow cytometry analysis, the Sample *Plecthranthus amboinicus* treated at 80µg/ml and 160µg/ml has induced early and late apoptosis in HepG2 with 7.57%, 18.36% and 5.17%, 20.25% apoptotic cells respectively. Necrotic cells were found to be 18.26% at 160µg/ml in Sample *P. amboinicus* respectively.

Gene regulation of BAX AND Bcl-2 in HEP-G2 cells treated with plant extracts

The gene expression analysis was designed to find the mechanism of apoptosis by evaluating the changes in the expression level of apoptosis-related genes. This study is important for the development of treatment strategies against liver cancer. Changes in expression level of apoptosis–related genes such as *BAX*, *BCL2* which had been treated with ethanolic leaves extract of *P. ambonicus* at concentrations of 80 and 160 μg/ml were investigated using Real Time PCR to investigate the mechanism of action. GAPDH was served as the housekeeping or internal control in all experiments.

The specific amplification of the expected products, according to primer design, was detection of a single distinctive band in agarose gel electrophoresis. Quantification of the results was accomplished by measuring the optical density of the bands, using the computerized imaging program Image J. The values were normalized to GAPDH intensity level. The Amplification of GAPDH gene in HEP-G2 is seen in figure 14. The amplification of BAX gene and Bcl 2 gene in HEP-G2 cells is seen in the figure 15 and figure 16.

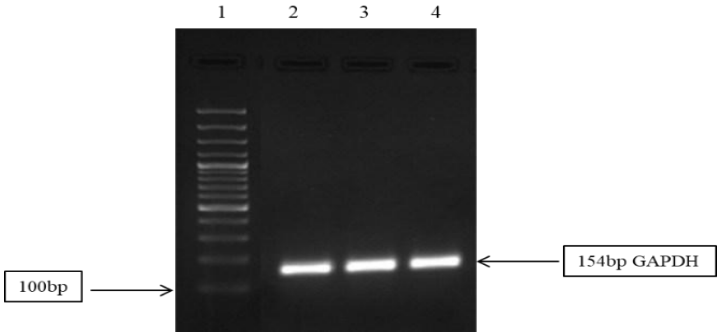

Figure 14: Amplification of GAPDH gene in HEP-G2 Lane 1-Ladder; lane 2–Control; Lane 3-80µg/ml; Lane 4-160µg/ml;

In the gel image fig 14 obtained from Chemidoc for GAPDH (internal control or housekeeping gene) it was found that the band was in the range of 154 bp thus it shows that RNA isolation is significantly done. In the fig 14 the intensity of GAPDH is same in all the three lanes indicating that the control and sample is having the same intensity.

ISSN No. 2454-6194 | DOI: 10.51584/IJRIAS |Volume XI Issue I January 2026

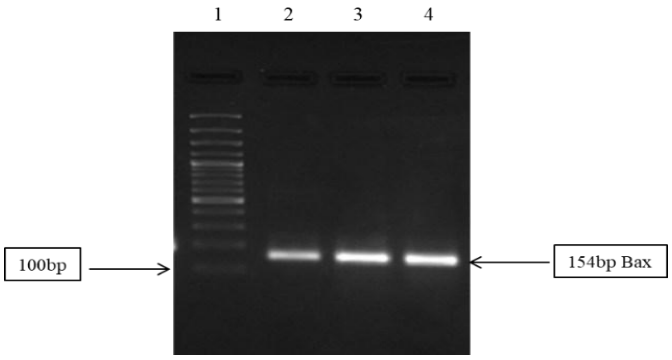

Figure 15: Amplification of BAX gene inHEP-G2 cells Lane 1-Ladder; lane 2–Control; Lane 3-80µg/ml; Lane 4-160µg/ml;

In the figure 15 band intensity obtained for control in lane 2 is slightly faint and as the concentration of the *Plecthranthus ambonicus* increases from the 80 to 160µg/ml in lane 3 and 4 the band intensity shown is comparatively brighter. Thus, indicating that the level of the bax expression is increased.

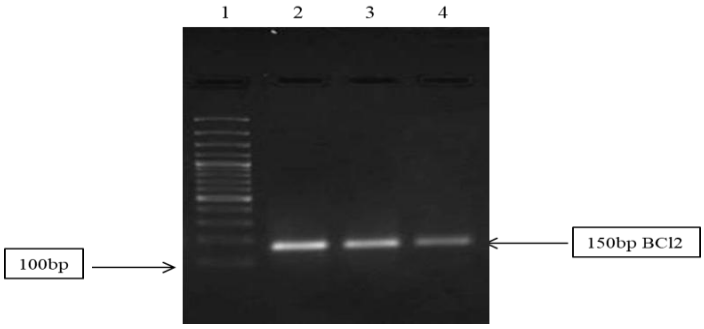

Figure 16: Amplification of BCL2 gene in HEP-G2.

Lane 1-Ladder; lane 2–Control; Lane 3-80µg/ml; Lane 4-160µg/ml;

In figure 16 the band intensity of control observed in lane 2 is slightly faint and as the concentration the *Plecthranthus ambonicus* increases from the 80 to 160µg/ml in lane 3 and 4 the band intensity shown is comparatively faint indicating decreased level of Bcl-2 expression.

Table 10: Relative expression of BAX gene inHEP-G2 cell line

Hep-G2 cells				
Sample Conc. µg/ml	**Band Intensity of PCR Amplicons IN watt/m²**		**Normalized**	**Relative Gene Expression**
	GAPDH	**BAX**		
0	38878.794	19422.56	0.50	1.00
80	39073.004	19936.83	0.51	1.02
160	37934.116	21031.93	0.55	1.11

Table 11: Relative expression of BCL2 gene in HEP-G2 cells.

Hep-G2 cells				
Sample Conc. µg/ml	**Band Intensity of PCR Amplicons IN watt/m²**		**Normalized**	**Relative Gene Expression**
	GAPDH	**BCl2**		
0	38878.794	34258.48	0.88	1.00
80	39073.004	27375.359	0.70	0.80
160	37934.116	16747.439	0.44	0.50

ISSN No. 2454-6194 | DOI: 10.51584/IJRIAS |Volume XI Issue I January 2026

Using Image J program, the band intensity for Bax and Bcl-2 in comparison with GAPDH band intensity is mentioned in table 10 and 11. The same program is used to normalize the values to GAPDH intensity levels where the program normalizes the intensity of GAPDH to 1 and using this the increasing and decreasing fold of relative gene expression for the concentrations 80 to 160µg/ml of the sample is detected.

The results indicate a significant increase in the relative expression levels of the BAX gene as the treatment concentration increased from 80 µg/ml to 160 µg/ml, with a fold change of 1.02 to 1.11 compared to the control, as depicted in bar graph 7. Additionally, the data clearly demonstrate a decreasing trend in Bcl-2 relative expression with increasing treatment concentrations, as shown in graph 8. Cells treated with the sample exhibited a fold change of 0.80 to 0.50.

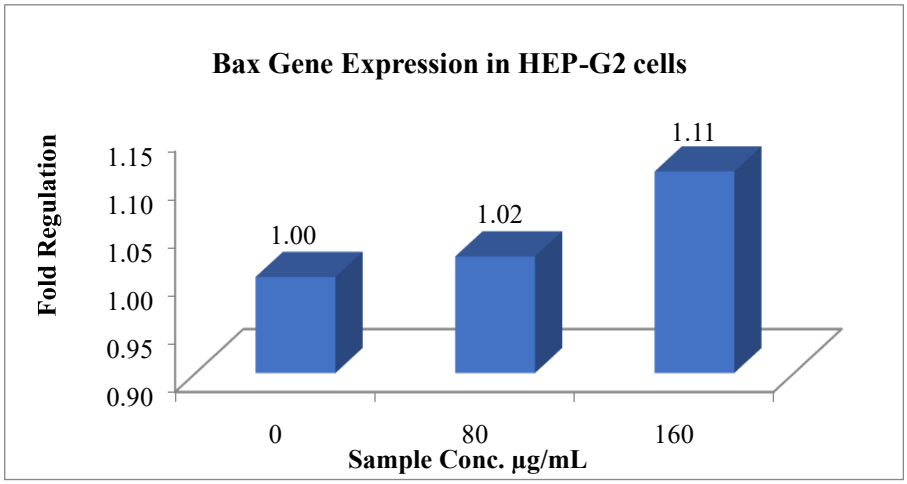

Graph 6: Bar graph representing Bax gene expression with sample concentration on x-axis and fold regulation on y-axis

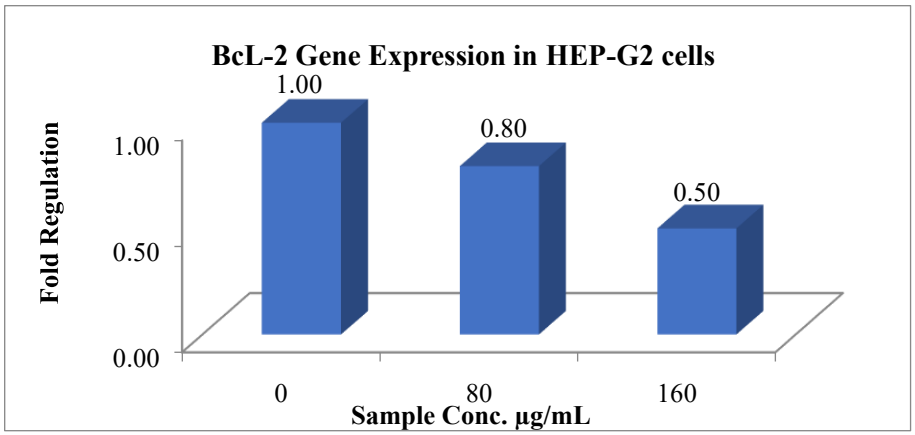

Graph 7: Bar graph representing Bcl-2 gene expression with sample concentration on x-axis and fold regulation on y-axis

DISCUSSION

Hepatocellular carcinoma (HCC) is a prevalent form of liver cancer, accounting for more than 90% of all primary liver malignancies globally [31]. The high incidence and mortality associated with HCC underscore the urgent need for the development of new chemo preventive agents that are both effective and free of significant side effects. The HepG2 cell line is widely utilized in research to study liver cancer due to its relevance as a model for HCC [32].

Medicinal plants are known for their diverse biological properties, including antitumor, antidepressant, antiinflammatory, antioxidant, antimicrobial, insecticidal, antifungal, antibacterial, anthelmintic, and antidiabetic activities [33]. Among these, *P. amboinicus* (Lour.) Spreng. and *H. rosa-sinensis* have attracted attention as potential alternative cancer therapies due to their low toxicity. However, their effects on apoptosis

in cancer cells have not been previously studied. Our research is the first to investigate the apoptotic potential of *P. amboinicus* and *H. rosa-sinensis* in HepG2 cells, marking a significant step forward in exploring these plants as sources of novel anticancer agents.

Cytotoxicity studies using the MTT assay demonstrated that the ethanolic leaf extracts of P. amboinicus and H. rosa-sinensis exhibit significant inhibitory effects on the HepG2 cell line, with P. amboinicus showing a notably higher percentage of inhibition. The IC50 values were determined to be 146.80 µg/ml for *P. amboinicus* and 278.20 µg/ml for *H. rosa-sinensis*, indicating that *P. amboinicus* possesses greater cytotoxic activity compared to the standard drug Doxorubicin, which had an IC50 of 18.26 µM. These findings align with observations by Shekh, R et al., 2022 who reported that the ethanol extract of *P. amboinicus* significantly impeded the viability of HepG2 cells at 400 µg/ml ($p < .01$) [34]. The results from our study also highlight a concentration-dependent increase in the inhibition of HepG2 cell growth, with maximum inhibition observed at the highest tested concentration of 100 µg/ml. These findings further support the potential of *P. amboinicus* as a promising source for developing therapeutic anticancer agents, consistent with previous studies that emphasize the role of traditional medicine in discovering effective treatments for cancer. The observed decrease in cell viability with increasing extract concentrations corroborates the cytotoxic effects of *P. amboinicus,* warranting additional investigations into its mechanisms and active compounds for potential clinical applications.

Following the cytotoxicity studies, an in vitro hemolytic activity assessment was conducted on human erythrocytes using ethanolic extracts from the leaves of *P. ambonicus* and *H. rosa-sinensis*. The hemolytic activity was evaluated at various concentrations (10, 20, 40, 80, 160, and 320 µg/ml), with results indicating that *P. ambonicus* exhibited a hemolytic activity range of 14-42%, while *H. rosa-sinensis* showed a range of 1745% at the same concentrations. Notably, both extracts demonstrated maximum hemolytic activity at the highest concentration of 320 µg/ml.The hemolytic activity observed is indicative of the extracts' potential to disrupt the lipid bilayer of red blood cells, a phenomenon that correlates with the concentration and potency of the extracts. While the hemolytic assays are crucial for evaluating the safety profile of these extracts, the results suggest that *H. rosa-sinensis* is considered safe for pharmacological use at lower concentrations (10, 20, and 40 µg/ml), as they induce less than 30% hemolysis. Conversely, concentrations of 80, 160, and 320 µg/ml are deemed toxic due to exceeding the 30% hemolysis threshold. In contrast, *P. ambonicus* remains within a safe range across all tested concentrations, as it consistently resulted in less than 30% hemolysis. These findings underscore the importance of evaluating hemolytic activity alongside cytotoxicity, as compounds with potent biological effects may pose risks if they also exhibit significant hemolytic properties. The relatively lower hemolytic activity of *P. ambonicus* suggests its potential for further exploration as a safer therapeutic agent, while the hemolytic profile of *H. rosa-sinensis* necessitates caution in its pharmacological application at higher concentrations. Overall, these results contribute valuable insights into the safety and efficacy of these plant extracts for potential therapeutic use.

Given the hemolytic results indicating potential toxicity at higher concentrations, *H. rosa-sinensis* will be excluded from further investigations involving flow cytometry to assess apoptotic potential, ensuring a focus on the safer extract of *P. ambonicus* for subsequent studies.

The apoptosis studies employed a dual staining technique using Acridine Orange (AO) and Ethidium Bromide (EtBr) to assess the ability of *P. ambonicus* extracts to induce apoptosis in HepG2 cell lines at concentrations of 80 µg/mL and 160 µg/mL. These concentrations were selected based on the hemolytic activity results, which indicated the extract activity approached the threshold but still remained within a safe margin, making these concentrations suitable for further investigations. The AO-EtBr results revealed distinct staining patterns that correspond to different stages of apoptosis. Early apoptotic cells exhibited yellow-green fluorescence due to AO staining, indicating chromatin condensation and nuclear fragmentation. This early stage of apoptosis suggests that the extract effectively initiates the apoptotic process. In contrast, late apoptotic cells were identified by orange fluorescence from EtBr staining, indicating a loss of membrane integrity and the presence of condensed, fragmented nuclei. Cells that fully incorporated EtBr were classified as necrotic, displaying altered nuclear morphology.The presence of early and late apoptotic cells indicates that *P. ambonicus* not only initiates apoptosis but also progresses through the apoptotic pathway, ultimately leading to cell death. These findings suggest that *P. ambonicus* extracts possess significant potential as an anticancer agent by effectively inducing apoptosis in HepG2 cells. The dual staining results provide compelling evidence of the extract's ability to trigger programmed cell death, supporting its further exploration as a therapeutic candidate in cancer treatment.

To quantitatively assess the induction of apoptosis in HepG2 cells treated with *P. ambonicus* extracts, flow cytometry was employed using Annexin V-FITC and propidium iodide (PI) staining. This method allows for the precise identification and quantification of viable, early apoptotic, late apoptotic, and necrotic cells based on their membrane integrity and the binding properties of the stains. The flow cytometry results indicated that treatment with *P. ambonicus* at concentrations of 80 µg/mL and 160 µg/mL led to the induction of early and late apoptosis. Specifically, the analysis revealed early apoptotic cell populations of 7.57% at 80 µg/mL and 5.17% at 160 µg/mL, while late apoptotic cells were observed at 18.36% and 20.25%, respectively. These findings suggest that the extract effectively triggers the apoptotic process in HepG2 cells, with a notable increase in late apoptotic cells at the higher concentration. The presence of necrotic cells was also noted, particularly at 160 µg/mL, where 18.26% of the cells were classified as necrotic. This indicates that while *P. ambonicus* induces apoptosis, there is also a degree of necrosis occurring at this concentration, which may reflect the cytotoxic effects of the extract. The results from the flow cytometry analysis corroborate the findings from the dual staining method, confirming that *P. ambonicus* not only inhibits cell growth but also induces apoptosis in a concentrationdependent manner. The ability of Annexin V to bind to phosphatidylserine (PS) exposed on the outer membrane of apoptotic cells provides a reliable indicator of early apoptotic events, while the combination with PI allows for the differentiation between late apoptotic and necrotic cells [35]. Overall, the flow cytometry results provide quantitative evidence of the pro-apoptotic effects of *P. ambonicus* on HepG2 cells, highlighting its potential as an effective anticancer agent. The observed induction of both early and late apoptosis, along with the presence of necrotic cells, underscores the extract's capacity to influence cell death pathways, warranting further investigation into its mechanisms of action and therapeutic applications.

To further elucidate the mechanisms underlying the apoptotic effects of *P. ambonicus* on HepG2 cells, gene expression analysis of the key apoptosis regulators, *BAX* and *BCL-2*, was conducted using real-time PCR (RTPCR). This analysis aimed to determine the changes in expression levels of these genes in response to treatment with *P. ambonicus* extracts at concentrations of 80 µg/mL and 160 µg/mL.The RT-PCR results revealed a marked increase in the relative expression levels of the pro-apoptotic *BAX* gene as the treatment concentration increased from 80 µg/mL to 160 µg/mL. The *BAX* gene expression showed a 1.02 to 1.11-fold increase compared to the control. In contrast, the relative expression of the anti-apoptotic *BCL-2* gene exhibited a decreasing trend, with cells treated with the extract showing a 0.80 to 0.50-fold reduction. These findings align with previous studies that reported regulated expression of Bcl-2 levels [34].

These findings suggest that the phytochemicals present in the *P. ambonicus* extract, such as saponins, terpenoids, and flavonoids, may contribute to its potent antioxidant and apoptotic activities. The downregulation of *BCL2* and upregulation of *BAX* expression indicate that the extract induces apoptosis by modulating the balance between pro- and anti-apoptotic genes in the *BCL-2* family. The *BCL-2* family proteins are key regulators of apoptosis, with *BCL-2* acting as an anti-apoptotic factor and *BAX* functioning as a pro-apoptotic factor [36].

When subjected to stress, such as treatment with the *P. ambonicus* extract, *BCL-2* may undergo conformational changes or be sequestered, leading to the release and activation of *BAX*. This shift in the *BAX/BCL-2* ratio ultimately tips the balance towards apoptosis, as evidenced by the increased expression of *BAX* and decreased expression of *BCL-2* in the treated cells.The results from the flow cytometry and RT-PCR analyses collectively demonstrate that the ethanolic extract of *P. ambonicus* effectively induces apoptosis in HepG2 cells through the overexpression of *BAX* and downregulation of *BCL-2*. These findings highlight the potential of *P. ambonicus* as a promising source for developing anticancer agents and warrant further investigations into its mechanisms of action and active compounds.

To advance the development of potential therapeutic agents, in vitro and in vivo models can be employed. In vitro models allow for large-scale screening of compounds to identify potential lead candidates, while in vivo models are crucial for evaluating the activity and efficacy of these compounds in a whole organism. Additionally, molecular modeling tools can be utilized to predict the binding interactions between compounds and target proteins, facilitating the identification of novel enzyme inhibitors and therapeutic agents.

In conclusion, the combined results from the cytotoxicity, hemolysis, flow cytometry, and gene expression analyses demonstrate the potent anticancer potential of *P. ambonicus* extract. The extract effectively induces apoptosis in HepG2 cells by modulating the expression of key apoptosis regulators, *BAX* and *BCL-2*, without significant hemolytic toxicity at lower concentrations. These findings provide a strong foundation for further investigations into the therapeutic applications of *P. ambonicus* in liver cancer treatment.

ISSN No. 2454-6194 | DOI: 10.51584/IJRIAS |Volume XI Issue I January 2026

CONCLUSION

Hepatocellular carcinoma (HCC) remains a significant global health challenge, necessitating the exploration of effective and safe therapeutic agents. This study investigated the anticancer potential of ethanolic leaf extracts from *P. amboinicus* and *H. rosa-sinensis* on HepG2 cell lines. The results demonstrated that *P.*

ambonicus exhibited superior cytotoxic activity, with an IC50 value of 146.80 µg/mL, compared to *H. rosasinensis* and the standard drug Doxorubicin. Further analyses revealed that *P. ambonicus* maintained a favorable safety profile, as its hemolytic activity remained below the 30% threshold across all tested concentrations. This allowed for the selection of 80 µg/mL and 160 µg/mL for subsequent apoptosis studies. Dual staining techniques confirmed that *P. ambonicus* effectively induced both early and late apoptosis in HepG2 cells, supported by flow cytometry results indicating significant apoptotic populations.Gene expression analysis demonstrated that *P. ambonicus* treatment led to increased expression of the pro-apoptotic *BAX* gene and decreased expression of the anti-apoptotic *BCL-2* gene, highlighting its mechanism of inducing apoptosis. These findings collectively underscore the potential of *P. ambonicus* as a promising source for developing anticancer agents, warranting further investigation into its active compounds and mechanisms of action. The study lays a strong foundation for future research aimed at harnessing the therapeutic potential of this medicinal plant in liver cancer treatment.

Conflicts of Interest

We have no conflicts of interest to disclose

ACKNOWLEDGMENT

I would like to express my deepest gratitude to Professor Bhargavi Rajarathinam for her invaluable guidance and support during the course of this research.

Disclosure

The data and materials in this manuscript have not been published elsewhere and are not under consideration by another journal.

Funding

This research received no external funding and was funded by the author [Imbaasree Rajavelu].

Author Contributions

Imbaasree Rajavelu performed the research, designed the study, analyzed the data, and wrote the article. Bhargavi Rajarathinam supervised the overall project.

Data Availability

The data used to support the findings of this study are available from the corresponding author upon request.

Informed Consent

Not applicable

Consent for publication

Not applicable

REFERENCES

1. Llovet, J. M., Kelley, R. K., Villanueva, A., Singal, A. G., Pikarsky, E., Roayaie, S., ... & Finn, R. S. (2021). Hepatocellular carcinoma. Nature reviews Disease primers, 7(1), 1-28.
2. Kouroumalis, E., Tsomidis, I., & Voumvouraki, A. (2023). Pathogenesis of hepatocellular carcinoma: the interplay of apoptosis and autophagy. Biomedicines, 11(4), 1166.

3. Shojaie, L., Iorga, A., & Dara, L. (2020). Cell death in liver diseases: a review. International journal of molecular sciences, 21(24), 9682.
4. Qian, S., Wei, Z., Yang, W., Huang, J., Yang, Y., & Wang, J. (2022). The role of BCL-2 family proteins in regulating apoptosis and cancer therapy. Frontiers in oncology, 12, 985363.
5. Mohammad, R. M., Muqbil, I., Lowe, L., Yedjou, C., Hsu, H. Y., Lin, L. T., ... & Azmi, A. S. (2015, December). Broad targeting of resistance to apoptosis in cancer. In Seminars in cancer biology (Vol. 35, pp. S78-S103). Academic Press.
6. Malla, R. R., Marni, R., & Chakraborty, A. (2022). ROS-mediated pathways: potential role in hepatocellular carcinoma biology and therapy. In Theranostics and Precision Medicine for the Management of Hepatocellular Carcinoma, Volume 2 (pp. 321-335). Academic Press.
7. Guo, J., Yan, W., Duan, H., Wang, D., Zhou, Y., Feng, D., ... & Qin, X. (2024). Therapeutic Effects of Natural Products on Liver Cancer and Their Potential Mechanisms. Nutrients, 16(11), 1642.
8. Manurung, K., Sulastri, D., Zubir, N., & Ilyas, S. (2020). In silico anticancer activity and in vitro antioxidant of flavonoids in Plectranthus amboinicus. Pharmacognosy Journal, 12(6s).
9. Amtaghri, S., Qabouche, A., Slaoui, M., & Eddouks, M. (2024). A comprehensive overview of Hibiscus rosa-sinensis L.: Its ethnobotanical uses, phytochemistry, therapeutic uses, pharmacological activities, and toxicology. Endocrine, Metabolic & Immune Disorders-Drug Targets (Formerly Current Drug TargetsImmune, Endocrine & Metabolic Disorders), 24(1), 86-115.
10. Złotek, U., Mikulska, S., Nagajek, M., & Świeca, M. (2016). The effect of different solvents and number of extraction steps on the polyphenol content and antioxidant capacity of basil leaves (Ocimum basilicum L.) extracts. Saudi journal of biological sciences, 23(5), 628-633.
11. Jamil, M., Mirza, B., Yasmeen, A., & Khan, M. A. (2012). Pharmacological activities of selected plant species and their phytochemical analysis. J Med Plants Res, 6(37), 5013-5022.
12. Pandey, A., & Tripathi, S. (2014). Concept of standardization, extraction and pre phytochemical screening strategies for herbal drug. Journal of Pharmacognosy and phytochemistry, 2(5), 115-119.
13. Tyagi, T. (2017). Phytochemical screening of active metabolites present in Eichhornia crassipes (Mart.) Solms and Pistia stratiotes (L.): Role in ethanomedicine. Asian Journal of Pharmaceutical Education and Research, 6(4), 40-56.
14. Sheel, R., Nisha, K., & Kumar, J. (2014). Preliminary phytochemical screening of methanolic extract of Clerodendron infortunatum. IOSR Journal of Applied Chemistry, 7(1), 10-13.
15. Ralte, V. (2014). Evaluation of phytochemical contents of Ipomoea cairica (L) Sweet–a qualitative approach. Science Vision, 14(3), 145-51.
16. Garg, P., & Garg, R. (2019). Phytochemical screening and quantitative estimation of total flavonoids of Ocimum sanctum in different solvent extract. Pharma Innov J, 8(2), 16-21.
17. Chaudhary, S., Singh, M. P., & Rawat, A. K. S. (2019). PHYTOCHEMICAL CHARACTERIZATION AND FUNCTIONAL PROPERTIES OF NATURALLY ISOLATED MUCILAGE FROM HIBISCUS CANNABINUS L., AS A POTENTIAL NATURAL PHARMACEUTICAL EXCIPIENT.
18. Kadam, P. V., Yadav, K. N., Shivatare, R. S., Bhilwade, S. K., & Patil, M. J. (2014). Comparative studies on fixed oil from Ocimum sanctum and Ocimum basillicum seeds. Inventi Rapid: Planta Activa, 2012(4), 1-5.
19. Rajkumar, V., Guha, G., & Kumar, R. A. (2011). Antioxidant and anti-neoplastic activities of Picrorhiza kurroa extracts. Food and chemical toxicology, 49(2), 363-369.
20. Van Meerloo, J., Kaspers, G. J., & Cloos, J. (2011). Cell sensitivity assays: the MTT assay. Cancer cell culture: methods and protocols, 237-245.
21. Denizot, F., & Lang, R. (1986). Rapid colorimetric assay for cell growth and survival: modifications to the tetrazolium dye procedure giving improved sensitivity and reliability. Journal of immunological methods, 89(2), 271-277.
22. Hoque, M., Dave, S., Gupta, P., & Saleemuddin, M. (2013). Oleic acid may be the key contributor in the BAMLET-induced erythrocyte hemolysis and tumoricidal action. PloS one, 8(9), e68390.
23. Sæbø, I. P., Bjørås, M., Franzyk, H., Helgesen, E., & Booth, J. A. (2023). Optimization of the hemolysis assay for the assessment of cytotoxicity. International journal of molecular sciences, 24(3), 2914.
24. Harboe, N. M. G. (1958). On myelomatosis. Acta Haematologica, 20(1-4), 27-33.
25. Kasibhatla, S., Amarante-Mendes, G. P., Finucane, D., Brunner, T., Bossy-Wetzel, E., & Green, D. R. (2006). Acridine orange/ethidium bromide (AO/EB) staining to detect apoptosis. Cold Spring Harbor Protocols, 2006(3), pdb-prot4493.

26. Koopman, G., Reutelingsperger, C. P., Kuijten, G. A., Keehnen, R. M., Pals, S. T., & Van Oers, M. H. (1994). Annexin V for flow cytometric detection of phosphatidylserine expression on B cells undergoing apoptosis.
27. Kříž, V., Pospíchalová, V., Mašek, J., Kilander, M. B. C., Slavík, J., Tanneberger, K., ... & Bryja, V. (2014). β-arrestin promotes Wnt-induced low density lipoprotein receptor-related protein 6 (Lrp6) phosphorylation via increased membrane recruitment of Amer1 protein. Journal of Biological Chemistry, 289(2), 1128-1141.
28. Hummon, A. B., Lim, S. R., Difilippantonio, M. J., & Ried, T. (2007). Isolation and solubilization of proteins after TRIzol® extraction of RNA and DNA from patient material following prolonged storage. Biotechniques, 42(4), 467-472.
29. Varkonyi-Gasic, E., Wu, R., Wood, M., Walton, E. F., & Hellens, R. P. (2007). Protocol: a highly sensitive RT-PCR method for detection and quantification of microRNAs. Plant methods, 3, 1-12.
30. SHOJAEI, S., & Keshavarz, H. (2014). Detection of acute toxoplasmosis: the genitally transmittable infection.
31. Liu, Z., Jiang, Y., Yuan, H., Fang, Q., Cai, N., Suo, C., ... & Chen, X. (2019). The trends in incidence of primary liver cancer caused by specific etiologies: results from the Global Burden of Disease Study 2016 and implications for liver cancer prevention. Journal of hepatology, 70(4), 674-683.
32. Kalaivani, S., Jayanthi, S., Revathi, K., & Chandrasekaran, R. (2024). Phytochemical profile of Euphorbia hirta plant extract and its in vitro anticancer activity against the liver cancer HepG2 cells. Vegetos, 37(2), 528-535.
33. Adewumi, O. A., Singh, V., & Singh, G. (2020). Chemical composition, traditional uses and biological activities of artemisia species. Journal of Pharmacognosy and Phytochemistry, 9(5), 1124-1140.
34. Shekh, R., Tiwari, R. K., Ahmad, A., Ahmad, I., Alabdallah, N. M., Saeed, M., ... & Bajpai, P. (2022). Ethanolic extract of Coleus aromaticus leaves impedes the proliferation and instigates apoptotic cell death in liver cancer HepG2 cells through repressing JAK/STAT cascade. Journal of Food Biochemistry, 46(10), e14368.
35. Bevers, E. M., & Williamson, P. L. (2016). Getting to the outer leaflet: physiology of phosphatidylserine exposure at the plasma membrane. Physiological reviews, 96(2), 605-645.
36. Arıcan, G. O., Çakır, O., Arıcan, E., Kara, T., Dağdeviren, O., & Arı, S. (2012). Effects of Geven root extract on proliferation of HeLa cells and bcl-2 gene expressions. African Journal of Biotechnology, 11(18), 4296-4304.